Solving the hypersingular boundary integral equation in three-dimensional acoustics using a regularization relationship

Zai You Yan, Kin Chew Hung,[a] and Hui Zheng
Institute of High Performance Computing, 1 Science Park Road #01-01 The Capricorn, Singapore Science Park II, Singapore 117528

(Received 2 August 2002; revised 2 January 2003; accepted 24 January 2003)

Regularization of the hypersingular integral in the normal derivative of the conventional Helmholtz integral equation through a double surface integral method or regularization relationship has been studied. By introducing the new concept of discretized operator matrix, evaluation of the double surface integrals is reduced to calculate the product of two discretized operator matrices. Such a treatment greatly improves the computational efficiency. As the number of frequencies to be computed increases, the computational cost of solving the composite Helmholtz integral equation is comparable to that of solving the conventional Helmholtz integral equation. In this paper, the detailed formulation of the proposed regularization method is presented. The computational efficiency and accuracy of the regularization method are demonstrated for a general class of acoustic radiation and scattering problems. The radiation of a pulsating sphere, an oscillating sphere, and a rigid sphere insonified by a plane acoustic wave are solved using the new method with curvilinear quadrilateral isoparametric elements. It is found that the numerical results rapidly converge to the corresponding analytical solutions as finer meshes are applied. © *2003 Acoustical Society of America.* [DOI: 10.1121/1.1560164]

PACS numbers: 43.40.Rj, 43.20.Rz, 43.20.Fn [EGW]

I. INTRODUCTION

Boundary element method based on the Helmholtz integral equation has long been applied for the analysis of acoustic radiation and scattering problems. Its significant advantages over other popular numerical techniques such as the finite difference and finite element method include a reduction of dimensionality of the problem by one, and an automatic satisfaction of the radiation boundary condition. However, the classical boundary element method for exterior acoustic problems fails to provide a unique solution at certain frequencies, which are the characteristics of the associated interior problem. The nonuniqueness is a purely mathematical problem arising from the boundary integral formulation rather than from the nature of the physical problem. A detailed description about the nonuniquness problem is presented in Ref. 1.

Several modified integral formulations have been developed to overcome the nonuniqueness problem. By far, the combined Helmholtz integral equation formulation (CHIEF) proposed by Schenck[2] in 1968 and the composite Helmholtz integral equation (CHIE) presented by Burton and Miller[3] in 1971 are the two most popular approaches. In the CHIEF method, Schenck[2] combined the surface Helmholtz integral equation with the interior Helmholtz integral equation to form an overdetermined system of equations, which was then solved using the least-squares procedure. Seybert *et al.*[4] provided a computational method based on the CHIEF method using isoparametric element formulation. Recently, Chen *et al.*[5] extended the CHIEF method to the combined Helmholtz exterior integral equation formulation to solve the interior problems. Although the CHIEF method is very simple to implement, it fails when the interior points are located on a nodal surface of the corresponding interior problem. To date, the selection of some suitable interior points still remains as a difficult problem. On the other hand, the CHIE method uses a linear combination of the Helmholtz integral equation and its normal derivative equation. It was proved that the linear combination of these two integral equations would yield a unique solution for all frequencies with a suitable complex combination coefficient, even if both the Helmholtz integral equation and its normal derivative equation suffer from the nonuniqueness problem. This method appears to be robust for numerical implementation. However, it suffers from a major drawback that hypersingular integral is involved in the normal derivative of the Helmholtz integral equation. Numerical techniques for computing nonsingular, nearly singular, and nearly hypersingular integrals can be found in the review paper by Tanaka *et al.*[6]

Burton and Miller[3] used a double surface integral method throughout the integral equation to reduce the order of the hypersingularity. Although such a technique results in numerically tractable kernels, it is computationally expensive to evaluate a double surface integral. The regularization techniques developed by Meyer *et al.*[7] and Terai[8] are valid for planar element only. Mathews[9] compared the double surface integral method[3] and the regularization technique[7] using quadratic quadrilateral isoparametric elements. It was noted that the regularization technique resulted in $1/r$ type singular integrals over the element near the point of singularity, even if a polar coordinate transformation was employed. Chien *et al.*[10] developed an approach to regularize such hypersin-

[a]Electronic mail: hungkc@ihpc.a-star.edu.sg

 0001-4966/2003/113(5)/2674/10/$19.00

gular integrals by employing certain known identities from the associated interior Laplace problems. Adaptive subdivision around singular points was needed in the numerical computation. Yang[11] successfully implemented this method in the study of acoustic scattering across a wide frequency range. Liu and Rizzo[12] developed a general form of the hypersingular boundary integral equation, which contained at most weakly singular integrals. This weakly singular form was derived by employing certain integral identities involving the static Green's function. Recently, Liu and Chen[13] made an improvement on this method with a new formulation that involves only tangential derivatives of the density function. Especially, C^0 continuous boundary elements were employed in the discretization. Wu *et al.*[14] implemented a regularized normal derivative equation, which converges in the Cauchy principal value sense rather than in the finite-part sense. This equation required the evaluation of tangential derivatives everywhere on the boundary. By taking the advantage of the properties of axisymmetric geometry, Wang *et al.*[15] successfully computed the hypersingular integrals using tangential operators. But this approach can only be applied to the problems with axisymmetric geometry. Hwang[16] regularized the hypersingular Helmholtz integral equation by some identities from the associated Laplace equations. The collocation points were chosen to be the Gauss–Legendre nodes and no interpolation function was assumed for acoustic variables. In that study, an important assumption was that the normal derivative of the dimensionless solid angle was identical to zero as point was on the surface. On the other hand, source distribution for the equipotential surface from the potential theory was employed to regularize the weak singularities. Therefore, the value of equipotential inside the domain must be calculated. A mathematical investigation about the existence of uniqueness theorems of the boundary element methods based on the Helmholtz integral equation was performed by Luke and Martin.[17] They also discussed the treatment of the hypersingular integral by the double surface integral method.

In this paper, the regularization of the hypersingular integral in the CHIE method is investigated through the double surface integral method. As stated earlier, it is computationally expensive to evaluate a double surface integral. Now by introducing the new concept of discretized operator matrix, evaluation of the double surface integral is reduced to the evaluation of the two discretized operator matrices. As a result, the computational cost for calculating CHIE is comparable to that of solving the conventional Helmholtz integral equation as the number of frequencies to be computed increases. This paper is organized into five sections. Following the Introduction, a detailed theoretical formulation of the governing equation for acoustic propagation in unbounded exterior domain is presented. Next, a discretization scheme for the surface boundary integral equations using a set of curvilinear quadrilateral isoparametric elements is discussed. A new concept of discretized operator matrix is introduced here. The double surface integral is discretized according to this new concept and the discretized operator matrix of the hypersingular integral operator N_0 is found. The hypersingularity in the integral operator N_k is eliminated using the operation $N_k - N_0$. Then, numerical calculations are performed for pulsating and oscillating sphere radiation and plane acoustic wave scattering from a rigid sphere. Three kinds of surface Helmholtz integral equations have been solved. They are the conventional Helmholtz integral equation (HIE), the normal derivative of the conventional Helmholtz integral equation (NDHIE), and the composite Helmholtz integral equation (CHIE). Finally a conclusion is drawn.

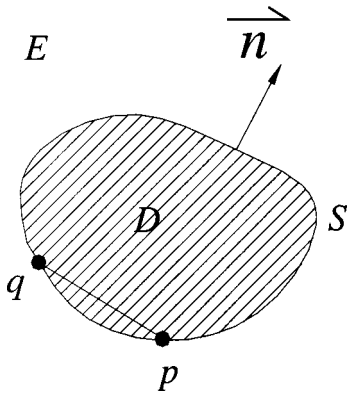

FIG. 1. Notation for a structure with smooth surface.

II. THEORETICAL DEVELOPMENT

Consider the acoustic pressure field in the exterior unbounded domain E. The acoustic field is either radiated by a finite body with smooth surface S vibrating with prescribed velocity distribution or scattered of acoustic waves from rigid surface S. The exterior infinite fluid medium is assumed to be homogeneous. Sound travels in the fluid medium with speed c and the fluid density is ρ. The normal vector at any point on the surface is taken to be the inward normal as shown in Fig. 1.

The governing differential equation[1] of the exterior acoustic domain in steady-state linear acoustics is the well-known Helmholtz equation,

$$(\nabla^2 + k^2)\varphi = 0. \tag{1}$$

The Neumann boundary condition on the boundary surface S can be expressed as

$$\frac{\partial \varphi}{\partial n} = i\omega\rho v_n. \tag{2}$$

In case of acoutic radiation, the acoustic pressure φ must satisfy the Sommerfeld radiation condition at infinity,

$$\lim_{r\to\infty} \int\int \left(\frac{\partial \varphi}{\partial r} + ikr\right)^2 dS = 0, \tag{3}$$

where φ represents the acoustic pressure, ω represents the circular frequency, k is the wave number, and v_n denotes the normal surface velocity.

By using the Green's second identity, the surface Helmholtz integral equation that satisfies the Sommerfeld radiation condition is

$$\int\int \left(\varphi(q) \frac{\partial G_k(p,q)}{\partial n_q} - G_k(p,q) \frac{\partial \varphi(p)}{\partial n_q} \right) dS_q = \frac{1}{2} \varphi(p). \tag{4}$$

The free-space Green's function G_k for the three-dimensional wave equation is

$$G_k(p,q) = e^{-ikr}/4\pi r, \quad r = |p-q|, \tag{5}$$

where p is the source point anywhere on the surface, and q is the field point on the surface, see Fig. 1. r represents the Euclidean distance between points p and q.

In operator notation,[8] Eq. (5) can be written as

$$\left[-\frac{1}{2} I + M_k \right] \varphi = L_k \frac{\partial \varphi}{\partial n}, \tag{6}$$

where

$$L_k \mu = \int\int \mu(q) G_k(p,q) dS_q, \tag{7}$$

$$M_k \mu = \int\int \mu(q) \frac{\partial G_k(p,q)}{\partial n_q} dS_q. \tag{8}$$

It is well known that the above surface Helmholtz integral equation, Eq. (4), leads to nonuniqueness solutions at certain frequencies that are the characteristics of the associated interior problem. As discussed in Sec. I, remedies to resolve the problem of nonuniqueness have been investigated by many researchers. Here, the CHIE method is studied.

The CHIE method is based on a linear combination of the surface Helmholtz integral equation, Eq. (4), and its normal derivative with respect to the source point. The resulting equation was proven to have unique solutions at all wave numbers, which can be expressed in operator notation as

$$\left\{ -\frac{1}{2} I + M_k + \alpha N_k \right\} \varphi = \left\{ L_k + \alpha \left[\frac{1}{2} I + M_k^T \right] \right\} \frac{\partial \varphi}{\partial n}, \tag{9}$$

where α, the coupling constant, is chosen to be strictly complex when wave number k is a real number. Here α takes the value $-i/k$. The integral operators N_k and M_k^T can be expressed as

$$\begin{aligned} N_k \mu &= \int\int \mu(q) \frac{\partial^2 G_k(p,q)}{\partial n_p \partial n_q} dS_q, \\ M_k^T \mu &= \int\int \mu(q) \frac{\partial G_k(p,q)}{\partial n_p} dS_q. \end{aligned} \tag{10}$$

The main drawback of the CHIE method is the numerical treatment of the hypersingular integral kernel N_k that appears in the normal derivative equation. Burton and Miller[3] used a regularization relationship, which replaces a hypersingular integral operator with two weakly singular integral operators, to deal with the hypersingularity in operator N_k. The regularization relationship used is

$$L_0 N_0 = [M_0 + \tfrac{1}{2} I][M_0 - \tfrac{1}{2} I] = M_0^2 - \tfrac{1}{4} I, \tag{11}$$

where L_0, N_0, and M_0 are integral operators identical to L_k, N_k, and M_k except that the kernels of L_0, N_0, and M_0 contain $G_0(p,q) = 1/4\pi r$ not G_k.

Therefore, the composite integral operators $L_0 N_0$ and M_0^2 are defined as

$$L_0 N_0 \mu(p) = \int\int G_0(p,q) \left\{ \int\int \frac{\partial^2 G_0(q,t)}{\partial n_q \partial n_t} \mu(t) dS_t \right\} dS_q, \tag{12}$$

$$M_0^2 \mu(p) = \int\int \frac{\partial G_0(p,q)}{\partial n_q} \left\{ \int\int \frac{\partial G_0(q,t)}{\partial n_t} \mu(t) dS_t \right\} dS_q. \tag{13}$$

According to the regularization relationship, Eq. (11), Burton and Miller[3] developed the following transformation to remove the hypersingularity in the operator N_k:

$$L_0 N_k = L_0[N_k - N_0] + L_0 N_0 = L_0[N_k - N_0] + M_0^2 - \tfrac{1}{4} I, \tag{14}$$

where

$$\begin{aligned} L_0[N_k - N_0]\mu(p) &= \int\int G_0(p,q) \\ &\quad \times \left[\int\int \frac{\partial^2 [G(q,t) - G_0(q,t)]}{\partial n_t \partial n_q} \mu(t) dS_t \right] dS_q. \end{aligned} \tag{15}$$

Then the CHIE in Eq. (9) was rewritten as

$$\begin{aligned} &L_0 \{ -\tfrac{1}{2} I - M_k + \alpha (N_k - N_0) \} \varphi + \alpha [M_0^2 - \tfrac{1}{4} I] \varphi \\ &\quad = L_0 \left\{ L_k + \alpha \left[\frac{1}{2} I + M_k^T \right] \right\} \frac{\partial \varphi}{\partial n}. \end{aligned} \tag{16}$$

In Eq. (16), the hypersingular integral operator N_k has been transformed into several weakly singular integral operators. However, the composite integral operators, such as $L_0[N_k - N_0]$ and M_0^2, are double surface integrals and these integrals must be computed for each frequency step. It is very inefficient to numerically implement such an approach. Therefore, even though it gives rise to tractable kernels, it is abandoned by most of the researchers. In this paper, the regularization relationship, Eq. (11), will be applied. A new method is proposed to discretize it. Finally a highly efficient approach is developed to solve the hypersingular integral.

III. DISCRETIZATION OF THE INTEGRAL OPERATORS

The integral operators are discretized using eight-noded, quadratic quadrilateral isoparametric surface elements which allows the integration of the interpolated variables over a three-dimensional surface to be carried out within a standard basis square in the (ξ, η) local coordinate space. The global Cartesian coordinates x are related to the nodal global coordinates x_i by

$$x(\xi, \eta) = \sum_{i=1}^{8} N_i(\xi, \eta) x_i. \tag{17}$$

$N_i(\xi, \eta)$ is the shape function[8] for the quadratic quadilateral elements with nodes numbered in counterclockwise fashion. The acoustic variables φ and $\partial\varphi/\partial n$ are approximated over each element by the shape functions, that is,

TABLE I. Comparison of computational time for different methods.

Model	Method	Per frequency step (s)	For N_0 operator (s)
24-element	Double surface integral [Eq. (16)]	148.751 67	x
	Proposed method [Eq. (35)]	1.081 555 2	0.751 080 0
	HIE [Eq. (6)]	1.041 497 7	x
96-element	Double surface integral [Eq. (16)]	8290.458	x
	Proposed method [Eq. (35)]	12.998 693	8.752 585
	HIE [Eq. (6)]	12.818 431	x

$$\varphi=\sum_{i=1}^{8} N_i\varphi_i, \quad \frac{\partial\varphi}{\partial n}=\sum_{i=1}^{8} N_i\frac{\partial\varphi_i}{\partial n}, \tag{18}$$

where φ_i represents the nodal quantity of the variable φ. With these relationships, integration of the integral operator L_k expressed in Eq. (7) can be discretized using n elements as follows:

$$\begin{aligned} L_k\varphi &= \int_S\int G_k(p,q)\varphi(q)dS_q \\ &= \sum_{j=1}^{n}\sum_{i=1}^{8}\int_{\Delta S_j}\int G_k(p,q)N_i(\xi,\eta)J(\xi,\eta)d\xi d\eta\varphi_i \\ &= B_k\{\varphi\}, \end{aligned} \tag{19}$$

where $\{\varphi\}=[\varphi_1,\varphi_2,\ldots K,\varphi_t]^T$, t is the total global node number. The square matrix B_k is defined as the discretized operator matrix of the integral operator L_k,

$$B_{ki,m}=\sum_{m=f(j,l)}\int_{\Delta S_j}\int N_l G_{kij}dS_q, \tag{20}$$

where the function $f(j,l)$ is the mapping function for the relation between element nodes and global nodes. Comparing Eq. (20) and Eq. (7), it is evident that the element of the discretized operator matrix takes the same integral form as the integral operator.

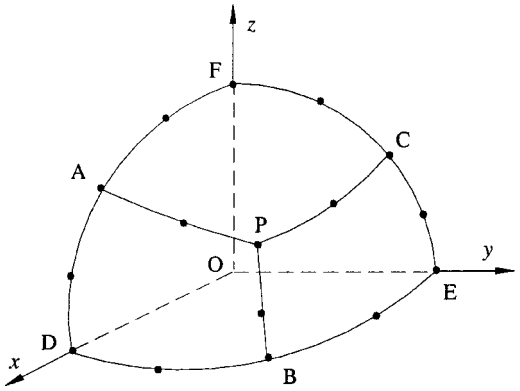

FIG. 2. Surface discretization of one octant of a sphere using 3 curvilinear quadrilateral elements.

Similarly, the discretized operator matrix A_k for the integral operator M_k is expressed as

$$A_{ki,m}=\sum_{m=f(j,l)}\int_{\Delta S_j}\int N_l\frac{\partial G_{kij}}{\partial n}dS_q, \tag{21}$$

and that for the discretized operator matrices B_0 and D_0 of the integral operators L_0 and N_0 are

$$\begin{aligned} B_{0i,m} &= \sum_{m=f(j,l)}\int_{\Delta S_j}\int N_l G_{0ij}(p,q)dS_q, \\ D_{0i,m} &= \sum_{m=f(j,l)}\int_{\Delta S_j}\int \frac{\partial^2 G_{0ij}(p,q)}{\partial n_p\partial n_q}N_l dS_q. \end{aligned} \tag{22}$$

In the past, the composite integral operator L_0N_0 in Eq. (12) was directly approximated as

$$\begin{aligned} L_0N_0\mu_i(p) &= \sum_{j=1}^{n}\int_{\Delta S_j}\int G_{0ij}(p,q) \\ &\quad\times\left\{\sum_{l=1}^{n}\int_{\Delta S_l}\int\frac{\partial^2 G_{0jl}(q,t)}{\partial n_q\partial n_t}\sum_{k=1}^{8}N_k\mu_k dS_t\right\}dS_q \\ &= \sum_{j=1}^{n}\sum_{l=1}^{n}\sum_{k=1}^{8}\int_{\Delta S_j}\int G_{0ij}(p,q) \\ &\quad\times\left\{\int_{\Delta S_l}\int\frac{\partial^2 G_{0jl}(q,t)}{\partial n_q\partial n_t}N_k dS_t\right\}dS_q\mu_k, \end{aligned} \tag{23}$$

which is obviously too computationally expensive to evaluate, and has deterred from implementing the regularization relationship, Eq. (11).

In this study, a new idea is proposed to discretized the composite integral operator L_0N_0. Assuming that

$$\psi(q)=\int_S\int\frac{\partial^2 G_0(q,t)}{\partial n_q\partial n_t}\mu(t)dS_t, \tag{24}$$

over each element, using the shape functions N_l, we have

$$\psi=\sum_{l=1}^{8}N_l\psi_l, \tag{25}$$

where ψ_l is nodal value of function ψ. Based on the definition of discretized operator matrix, Eq. (24) can be dis-

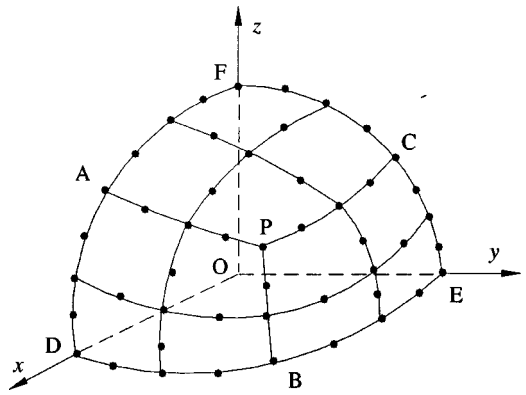

FIG. 3. Surface discretization of one octant of a sphere using 12 curvilinear quadrilateral elements.

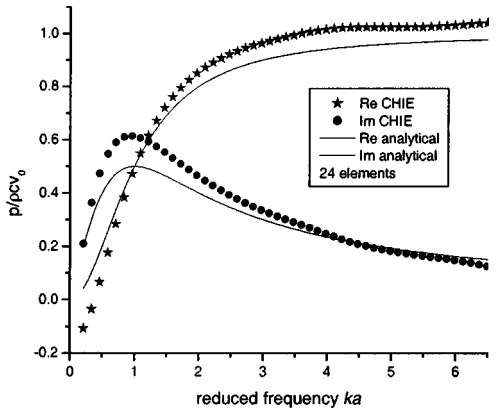

FIG. 5. Dimensionless surface acoustic pressures from a pulsating sphere using CHIE with 24 elements.

cretized and expressed in the form of discretized operator matrix,

$$\{\psi\}=D_0\{\mu\}, \tag{26}$$

where $\{\psi\}$ and $\{\mu\}$ are values at global nodes, and are constants in the integration. D_0 is the discretized operator matrix of integral operator N_0. Because N_0 is a hypersingular integral operator and the integral does not exist in either conventional or Cauchy-principal value sense. The operator matrix D_0 should be obtained in the Hadamard finite part sense.[16]

Substituting Eq. (24) into Eq. (12), we have

$$L_0N_0\mu(p)=\int\int_S G_0(p,q)\psi(q)dS_q. \tag{27}$$

The discretization of Eq. (27) can be expressed in discretized operator matrix form as

$$E_0\{\mu\}=B_0\{\psi\}, \tag{28}$$

where E_0 is the discretized operator matrix of the composite integral operator L_0N_0. Substituting Eq. (26) into Eq. (28), we have

$$E_0\{\mu\}=B_0D_0\{\mu\}. \tag{29}$$

Because the regularization relationship, Eq. (11), is an identity formulation and μ is an arbitrary function, the discretized operator matrix E_0 is equal to the product of B_0 and D_0,

$$E_0=B_0D_0. \tag{30}$$

The discretized operator matrix A_0^2 corresponding to the composite integral operator M_0^2 can be obtained in the same way. A_0 is the discretized operator matrix of integral operator M_0,

$$A_{0,im}=\sum_{m=f(j,l)}\int\int_{\Delta S_j}N_l\frac{\partial G_{0ij}}{\partial n}dS_q. \tag{31}$$

Therefore, the regularization relationship, Eq. (11), can be expressed in the form of discretized operator matrices as

$$B_0D_0=A_0^2-\tfrac{1}{4}I. \tag{32}$$

Then, we have

$$D_0=B_0^{-1}(A_0^2-\tfrac{1}{4}I). \tag{33}$$

Now the double surface integrations in the regularization relationship, Eq. (11), have been reduced to the product of surface integrations. Above all, the discretized operator matrix of the hypersingular integral operator N_0 as higher-order elements are implemented is explicitly found for the first time.

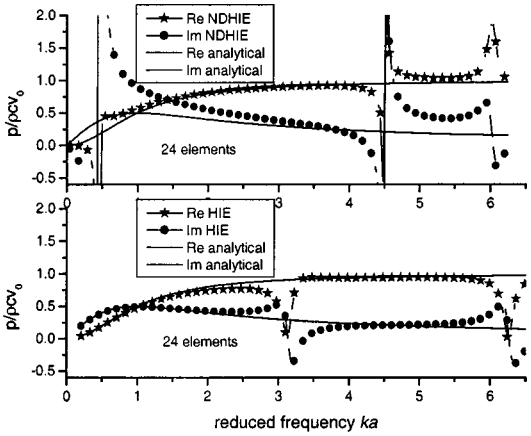

FIG. 4. Dimensionless surface acoustic pressures from a pulsating sphere using HIE and NDHIE with 24 elements.

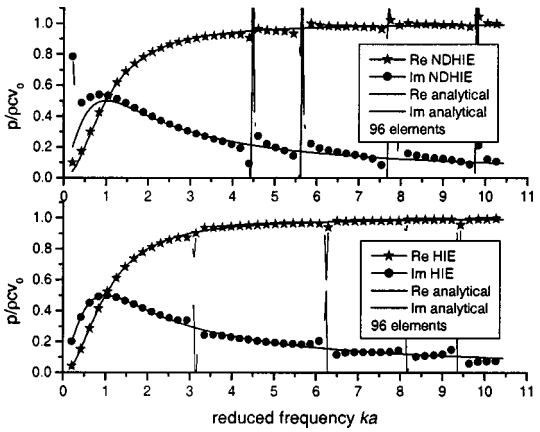

FIG. 6. Dimensionless surface acoustic pressures from a pulsating sphere using HIE and NDHIE with 96 elements.

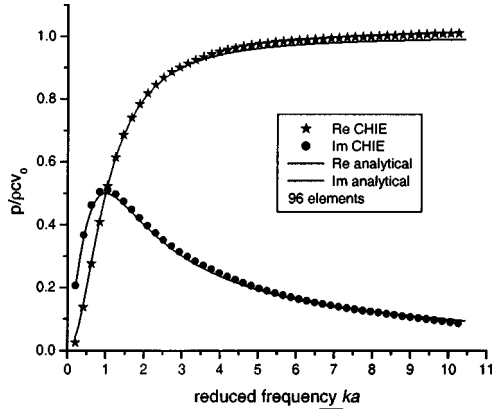

FIG. 7. Dimensionless surface acoustic pressures from a pulsating sphere using CHIE with 96 elements.

IV. TREATMENT OF THE HYPERSINGULARITY IN OPERATOR N_k

Now applying the integral operator N_0, Eq. (9) can be modified as

$$[-\tfrac{1}{2}I+M_k+\alpha[(N_k-N_0)+N_0]]\varphi = \left[L_k+\alpha\left[\frac{1}{2}I+M_k^T\right]\right]\frac{\partial\varphi}{\partial n}. \tag{34}$$

The term (N_k-N_0) has removed the hypersingularity in operator N_k. Only the term N_0 still contains hypersingularity. Using the discretized operator matrices, Eq. (34) can be discretized and expressed as

$$\left[-\frac{1}{2}I+A_k+\alpha[D+D_0]\right]\{\varphi\}=\left[B_k+\alpha\left[\frac{1}{2}I+F\right]\right]\left\{\frac{\partial\varphi}{\partial n}\right\}, \tag{35}$$

where D is the discretized operator matrix for integral operator (N_k-N_0) and F is the discretized operator matrix of integral operator M_k^T,

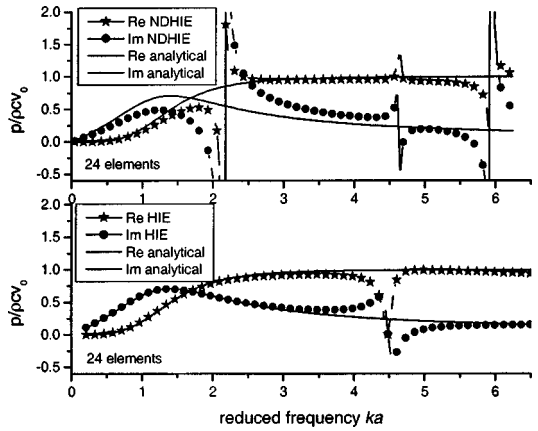

FIG. 8. Dimensionless surface acoustic pressures for an oscillating sphere using HIE and NDHIE with 24 elements as $\theta=0°$.

$$D_{im}=\sum_{m=f(j,l)}\int\int_{\Delta S_j} N_l\frac{\partial^2(G_{kij}-G_{0ij})}{\partial n_t\partial n_q}dS_q,$$
$$F_{im}=\sum_{m=f(j,l)}\int\int_{\Delta S_j} N_l\frac{\partial G_{0ij}(p,q)}{\partial n_p}dS_q. \tag{36}$$

Since the discretized operator matrix D_0 of the hypersingular integral operator N_0 has already been obtained by Eq. (33), the linear equation system in Eq. (35) can be numerically solved using a weakly singular integration scheme, such as that proposed by Lachat and Watson.[18]

As the discretized operator matrix D_0 is independent of frequency, the computational cost of solving Eq. (35) is comparable to that of solving the conventional Helmholtz integral equation, Eq. (6), as the number of frequencies to be computed increases. Table I presents the computational time for solving the problem of pulsating sphere radiation, which will be described in detail in Sec. V, using different methods. Here the computer is a Dell Latitude C610 notebook. Clearly, the new approach greatly improves the computational efficiency as compared to the technique applied in Eq. (16). For each frequency step, the computational time for the new method is very close to that for the HIE Eq. (6).

V. NUMERICAL EXAMPLES

In order to test the accuracy and efficiency of the new method, two cases of acoustic radiation and a case of plane acoustic wave scattering from rigid sphere have been computed. The two acoustic radiation problems are pulsating sphere radiation and oscillating sphere radiation. In all three examples, the surface of a sphere is, respectively, modeled using 24 and 96 curvilinear quadrilateral isoparametric elements to observe the convergence of the new method. Each octant of a sphere is discretized using 3 and 12 surface elements as shown in Figs. 2 and 3. Due to symmetry, the problems are computed in half space. For radiation problems, three linear equation systems are computed. They are the conventional Helmholtz integral equation (HIE), normal derivative equation of the conventional Helmholtz integral equation (NDHIE), and the composite Helmholtz integral equation (CHIE). Comparisons between the numerical results of these three linear equation systems clearly show the nonuniqueness problem and the effectiveness of the new method. For plane acoustic wave scattering from a rigid sphere, only the conventional Helmholtz integral equation and the composite Helmholtz integral equation are computed. These examples are computed using the in-house developed code, SSFI. This software is suitable to solve multi-domain acoustic problems, especially the problems of structural–acoustic interaction.

A. Pulsating sphere radiation

The analytical solution[10] of the acoustic pressure $\varphi(r)$ for a sphere of radius a, pulsating with an uniform radial velocity v_0, is given by

$$\frac{\varphi(r)}{\rho c v_0}=\frac{a}{r}\frac{ika}{1+ika}e^{-ik(r-a)}. \tag{37}$$

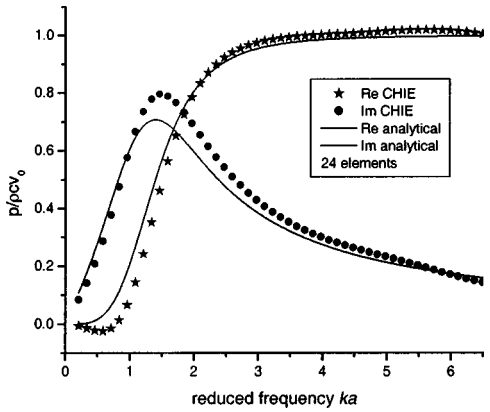

FIG. 9. Dimensionless surface acoustic pressures for an oscillating sphere using CHIE with 24 elements as $\theta=0°$.

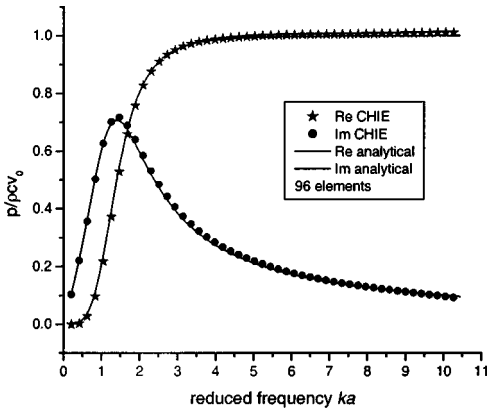

FIG. 11. Dimensionless surface acoustic pressures for an oscillating sphere using CHIE with 96 elements as $\theta=0°$.

Dimensionless surface acoustic pressures as a function of the reduced frequency *ka* are plotted in Figs. 4–7. Figures 4 and 5 present the results obtained using 24 elements. While the numerical results obtained using 96 elements are presented in Figs. 6 and 7. The comparison between the numerical results obtained using the HIE and NDHIE with the corresponding analytical solutions is shown in Figs. 4 and 6. It is evident that the HIE equation fails to provide unique solutions near $ka=\pi$, 2π, 8.13, and 3π and the NDHIE equation fails to provide unique solutions near $ka=0$, 4.493, 5.616, 7.725, and 9.784. On the other hand, the numerical results calculated using the CHIE, which are plotted in Figs. 5 and 7, are unique for all the frequencies. Figure 7 shows that with a finer mesh, the numerical results obtained using the CHIE agree very well with the analytical solutions for *ka* up to 10.5.

B. Oscillating sphere radiation

The analytical solution[10] of the acoustic pressure for an oscillating sphere of radius a with a radial velocity $v_0\cos(\theta)$ is given by

$$\frac{\varphi(r)}{\rho c v_0}=\left(\frac{a}{r}\right)^2\cos(\theta)\frac{ika(1+ikr)}{2(1+ika)-k^2a^2}e^{-ik(r-a)}, \qquad (38)$$

where θ is the angle made by the radial direction and the direction of the velocity. In the following example, $\theta=0$ is along the direction of z axis.

The dimensionless surface acoustic pressures at $\theta=0$ are displayed as function of the reduced frequency in Figs. 8–11. Figures 8 and 9 show the results obtained using the model with 24 elements. The results for 96 elements model are shown in Figs. 10 and 11. The comparison between the numerical results obtained using the HIE and NDHIE with the corresponding analytical solutions is shown in Figs. 8 and 10. As can be seen, the HIE equation fails to provide unique solutions near $ka=4.493$, 7.725, and 9.349. Similarly, the NDHIE equation also suffers from the nonuniqunness near $ka=2.062$, 5.911, 5.616, 6.787, 8.521, and 9.150, whereas the numerical results calculated using the CHIE displayed in Figs. 9 and 11 are unique for all the wave numbers. Figure 11 shows that with a finer mesh discretization the surface acoustic pressures for an oscillating sphere obtained using the CHIE agree quite well with the corresponding analytical solutions for *ka* up to 10.5.

C. Plane acoustic wave scattering from a rigid sphere

To provide a further test of the new technique, the scattering of a plane acoustic wave $\varphi_I=\varphi_0 e^{-ikz}$ from a rigid sphere of radius a is computed. The analytical solution[19] of

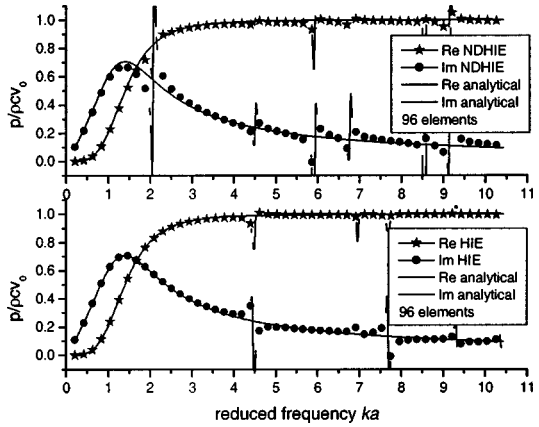

FIG. 10. Dimensionless surface acoustic pressures for an oscillating sphere using HIE and NDHIE with 96 elements as $\theta=0°$.

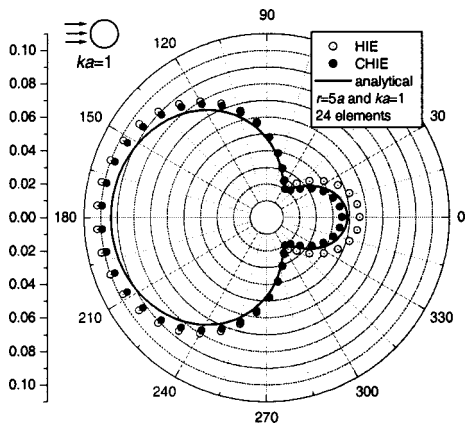

FIG. 12. The angular dependence of φ_s/φ_0 as $ka=1.0$ and $r=5a$ with 24 elements.

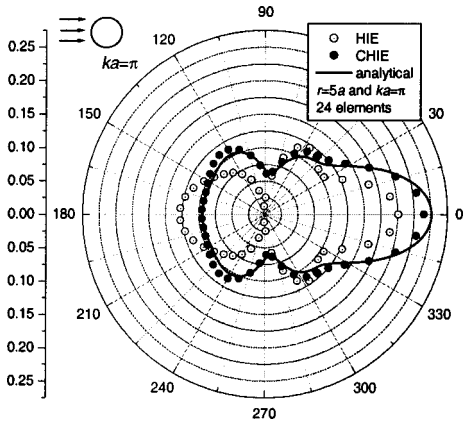

FIG. 13. The angular dependence of φ_s/φ_0 as $ka=\pi$ and $r=5a$ with 24 elements.

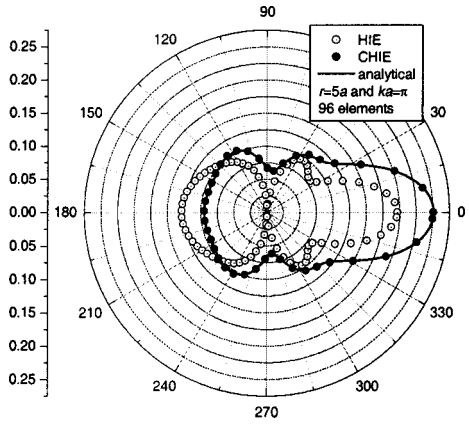

FIG. 16. The angular dependence of φ_s/φ_0 as $ka=\pi$ and $r=5a$ with 96 elements.

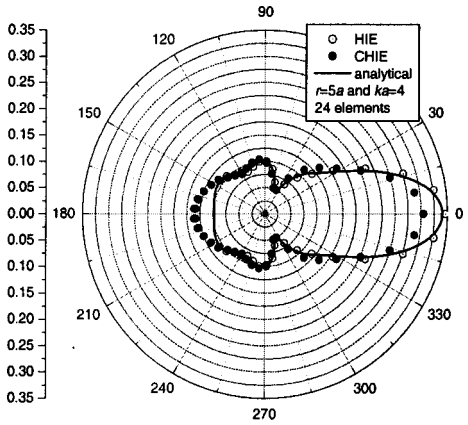

FIG. 14. The angular dependence of φ_s/φ_0 as $ka=4$ and $r=5a$ with 24 elements.

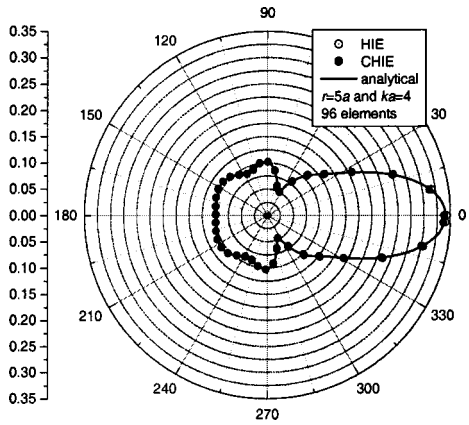

FIG. 17. The angular dependence of φ_s/φ_0 as $ka=4$ and $r=5a$ with 96 elements.

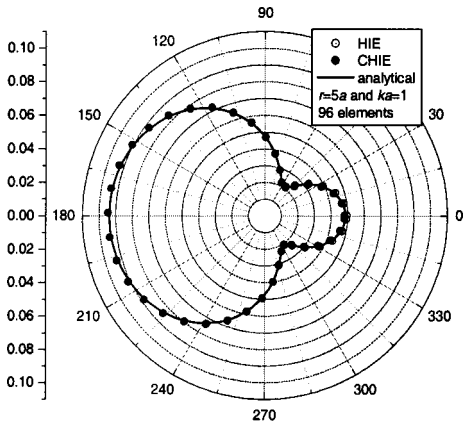

FIG. 15. The angular dependence of φ_s/φ_0 as $ka=1.0$ and $r=5a$ with 96 elements.

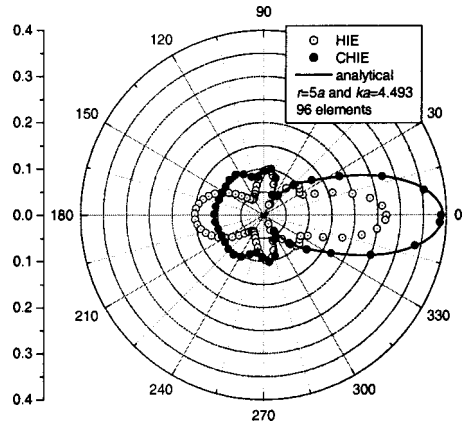

FIG. 18. The angular dependence of φ_s/φ_0 as $ka=4.493$ and $r=5a$ with 96 elements.

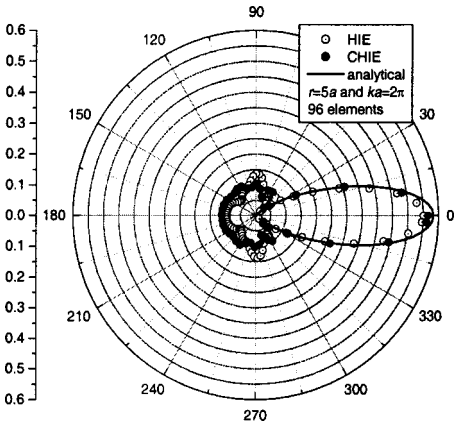

FIG. 19. The angular dependence of φ_s/φ_0 as $ka=2\pi$ and $r=5a$ with 96 elements.

the scattered acoustic pressure $\varphi_s(r,\theta)$ at a distance r from the center of the sphere and at an angle θ from the direction of the incoming wave is given by

$$\frac{\varphi_s(r,\theta)}{\varphi_0}=\sum_{m=0}^{\infty}\left[-(-i)^m(2m+1)\frac{j_m'(ka)}{h_m'(ka)}\right]h_m(kr)\times P_m(\cos\theta), \tag{39}$$

where j_m is spherical Bessel function of the first kind and h_m is spherical Hankel function of the second kind. P_m denotes Legendre polynomial of order m.

Figures 12–14 present the results obtained using the 24-element model. While Figs. 15–19 present the results obtained using the 96-element model. The results at $r=5a$ are presented. Figures 12 and 15 show the angular dependency of φ_s/φ_0 as $ka=1.0$. It is observed that the numerical results obtained using both the HIE and CHIE agree well with the analytical solutions. Figures 13 and 16 show the results at the reduced frequency $ka=\pi$. As $ka=\pi$ is one of the characteristic frequencies,[11] the scattered acoustic pressures obtained using the HIE do not agree with the corresponding analytical solutions. However, the scattered acoustic pressures obtained using the CHIE again agree very well with the analytical solutions. Figures 14 and 17 demonstrate the angular dependency of φ_s/φ_0 at $ka=4$. Comparisons between these two figures indicate that the numerical results converge rapidly as finer meshes are applied. Angular dependencies of φ_s/φ_0 at $ka=4.493$ and 2π are presented in Figs. 18 and 19, respectively. These frequencies correspond to the characteristic frequencies of either the conventional Helmholtz integral equation or its normal derivative equation. All these figures demonstrate that the new technique can overcome the nonuniqueness problem encountered in acoustic scattering analysis using the conventional Helmholtz integral equation.

VI. CONCLUSIONS

By introducing the concept of discretized operator matrix, a new method has been generated to overcome the hypersingular integral involved in the composite Helmholtz integral equation proposed by Burton and Miller.[3] The discretized operator matrix of a composite integral operator is proved to be just the product of the two discretized operator matrices corresponding to the two integral operators, which construct the composite integral operator. The double surface integrals employed by Burton and Miller[3] are discretized according to this new concept. Above all, the discretized operator matrix of the hypersingular integral operator N_0 is explicitly found for the first time as higher-order elements are implemented. Subsequently, an elimination of the hypersingularity in the integral operator N_k is implemented using the formulation N_k-N_0. The new method greatly improves the computational efficiency and has tractable integral kernels. Numerical calculations are performed for pulsating and oscillating sphere radiation and plane acoustic wave scattering from a rigid sphere with curvilinear quadrilateral isoparametric elements being employed. As finer meshes are applied, the numerical results agree quite well with the corresponding analytical solutions. Here surface of the object is constrained to be smooth enough. Further investigations will extend the new technique to problems with arbitrary shape structure.

[1] R. D. Ciskowski and C. A. Brebbia, *Boundary Element Methods in Acoustics* (Computational Mechanics, Souththampton, Boston, 1991).
[2] H. A. Schenck, "Improved integral formulation for acoustic radiation problems," J. Acoust. Soc. Am. **44**, 41–58 (1968).
[3] A. J. Burton and G. F. Miller, "The application of integral equation methods to the numerical solution of some exterior boundary value problems," Proc. R. Soc. London, Ser. A **323**, 201–210 (1971).
[4] A. F. Seybert, B. Soenarko, F. J. Rizzo, and D. J. Shippy, "An advanced computational method for radiation and scattering of acoustic waves in three dimensions," J. Acoust. Soc. Am. **77**, 362–368 (1985).
[5] I. L. Chen, J. T. Chen, S. R. Kuo, and M. T. Liang, "A new method for true and spurious eigensolutions of arbitrary cavities using the combined Helmholtz exterior integral equation formulation method," J. Acoust. Soc. Am. **109**, 982–998 (2001).
[6] M. Tanaka, V. Sladek, and J. Sladek, "Regularization techniques applied to boundary element methods," Appl. Mech. Rev. **47**, 457–499 (1994).
[7] W. L. Meyer, W. A. Bell, and B. T. Zinn, "Boundary integral solutions of three dimensional acoustic radiation problems," J. Sound Vib. **59**, 245–262 (1978).
[8] T. Terai, "On calculation of sound fields around three dimensional objects by integral equation methods," J. Sound Vib. **69**, 71–100 (1980).
[9] I. C. Mathews, "Numerical techniques for three dimensional steady-state fluid-structure interaction," J. Acoust. Soc. Am. **79**, 1317–1325 (1986).
[10] C. C. Chien, H. Rajiyah, and S. N. Atluri, "An effective method for solving the hyper-singular integral equations in 3-D acoustics," J. Acoust. Soc. Am. **88**, 918–937 (1990).
[11] S.-A. Yang, "Acoustic scattering by a hard and soft body across a wide frequency range by the Helmholtz integral equation method," J. Acoust. Soc. Am. **102**, 2511–2520 (1997).
[12] Y. J. Liu and F. J. Rizzo, "A weakly-singular form of the hypersingular boundary integral equation applied to 3-D acoustic wave problems," Comput. Methods Appl. Mech. Eng. **96**, 271–287 (1992).
[13] Y. J. Liu and S. H. Chen, "A new form of the hypersingular boundary integral equation for 3-D acoustics and its implementation with C0 boundary elements," Comput. Methods Appl. Mech. Eng. **173**, 375–386 (1999).
[14] T. W. Wu, A. F. Seybert, and G. C. Wan, "On the numerical implementation of a Cauchy principal value integral to insure a unique solution for acoustic radiation and scattering," J. Acoust. Soc. Am. **90**, 554–560 (1991).
[15] W. P. Wang, N. Atalla, and J. Nicolas, "A boundary integral approach for acoustic radiation of axisymmetric bodies with arbitrary boundary conditions valid for all wave numbers," J. Acoust. Soc. Am. **101**, 1468–1478 (1997).

[16] W. S. Hwang ''Hyper-singular boundary integral equations for exterior acoustic problems,'' J. Acoust. Soc. Am. **101**, 3336–3342 (1997).
[17] C. J. Luke and P. A. Martin, ''Fluid-solid interaction: Acoustic scattering by a smooth elastic obstacle,'' SIAM (Soc. Ind. Appl. Math.) J. Appl. Math. **55**, 904–922 (1995).
[18] J. C. Lachat and J. O. Watson, ''Effective numerical treatment of boundary integral equations,'' Int. J. Numer. Methods Eng. **10**, 991–1005 (1976).
[19] M. C. Junger, ''Sound scattering by thin elastic shells,'' J. Acoust. Soc. Am. **24**, 366–373 (1952).